EDGE ARTICLE

Check for updates

Stereoregular functionalized polysaccharides *via* cationic ring-opening polymerization of biomass-derived levoglucosan†

Mayuri K. Porwal, [a] Yernaidu Reddi, ‡[b] Derek J. Saxon, ‡[b] Christopher J. Cramer, [bc] Christopher J. Ellison *[a] and Theresa M. Reineke *[b]

We report the facile synthesis and characterization of 1,6-α linked functional stereoregular polysaccharides from biomass-derived levoglucosan *via* cationic ring-opening polymerization (cROP). Levoglucosan is a bicyclic acetal with rich hydroxyl functionality, which can be synthetically modified to install a variety of pendant groups for tailored properties. We have employed biocompatible and recyclable metal triflate catalysts – scandium and bismuth triflate – for green cROP of levoglucosan derivatives, even at very low catalyst loadings of 0.5 mol%. Combined experimental and computational studies provided key kinetic, thermodynamic, and mechanistic insights into the cROP of these derivatives with metal triflates. Computational studies reveal that ring-opening of levoglucosan derivatives is preferred at the 1,6 anhydro linkage and cROP proceeds in a regio- and stereo-specific manner to form 1,6-α glycosidic linkages. DFT calculations also show that biocompatible metal triflates efficiently coordinate with levoglucosan derivatives as compared to the highly toxic PF_5 used previously. Post-polymerization modification of levoglucosan-based polysaccharides is readily performed *via* UV-initiated thiol–ene click reactions. The reported levoglucosan based polymers exhibit good thermal stability (T_d > 250 °C) and a wide glass transition temperature (T_g) window (<−150 °C to 32 °C) that is accessible with thioglycerol and lauryl mercaptan pendant groups. This work demonstrates the utility of levoglucosan as a renewably-derived scaffold, enabling facile access to tailored polysaccharides that could be important in many applications ranging from sustainable materials to biologically active polymers.

Introduction

Polymers are indispensable in modern life and the global economy; however, more than 90% of current synthetic polymers are derived from fossil fuels and 87% of these produced polymers contribute to plastic waste, usually after a single use.[1–4] Lignocellulosic biomass is one of the most promising renewable feedstocks for sustainable polymers due to its worldwide abundance and availability.[5–10] The major component of lignocellulosic biomass is cellulose, and thermochemical conversion processes—such as fast pyrolysis—provide an efficient route to convert biomass cellulose into renewable chemicals.[5–8] The major product of cellulose fast pyrolysis is levoglucosan (Fig. 1A), which can be obtained with yields as

high as 80%.[11–14] Not surprisingly, levoglucosan has been identified as a building block for high value-added chemicals, pharmaceuticals, and surfactants.[13–15] As a result, there has been increasing interest in the commercial production of levoglucosan from biomass. Techno-economic analyses indicate that levoglucosan could be produced by thermochemical conversion at a low cost of $1.33 per kg to $3.0 per kg, which is competitive with many petroleum-derived monomers.[12,15–17]

Structurally, levoglucosan is an attractive feedstock for the synthesis of sustainable polymers. This anhydrosugar contains a bicyclic acetal linkage (Fig. 1A, highlighted in orange) that is amenable to cationic ring-opening polymerization (cROP).[18] Levoglucosan also offers rich functionality due to its three hydroxyl groups, which can be synthetically modified prior to cROP to install a variety of pendant groups for tailored properties. Furthermore, the incorporation of the rigid glucopyranose ring in the polymer backbone *via* cROP can increase the thermal stability of levoglucosan based polysaccharides.[19] Stereoregular polysaccharides are also of interest in biological and biomedical applications such as drug delivery and blood anti-coagulation due to their biocompatibility, multiple functionalities, and stereochemistry dependent properties.[20–24] In addition, stereoselective cROP of levoglucosan to obtain

*a*Department of Chemical Engineering and Materials Science, University of Minnesota, Minneapolis, Minnesota 55455, USA. E-mail: porwa001@umn.edu; cellison@umn.edu

*b*Department of Chemistry, University of Minnesota, Minneapolis, Minnesota 55455, USA. E-mail: treineke@umn.edu

*c*Underwriters Laboratories Inc., 333 Pfingsten Rd., Northbrook, Illinois 60620, USA

† Electronic supplementary information (ESI) available. See DOI: 10.1039/d2sc00146b

‡ Co-second authors.
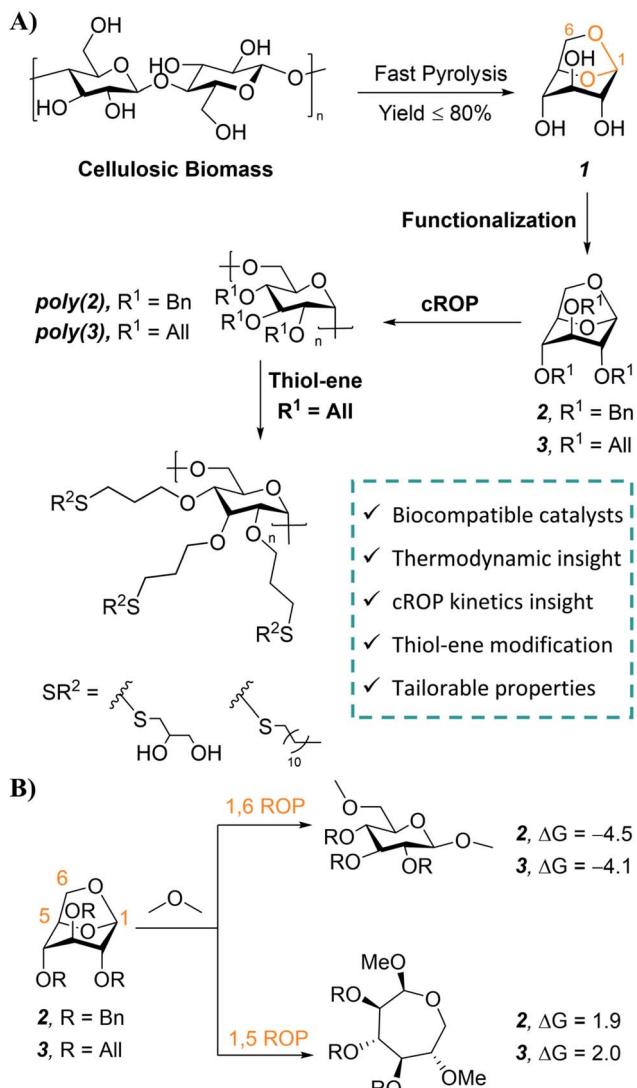
Fig. 1 (A) Schematic depicting synthesis of levoglucosan (**1**) from cellulosic biomass *via* fast pyrolysis. In this work, tribenzyl (**2**) and triallyl levoglucosan monomers (**3**) are subjected to metal triflate catalyzed cROP to synthesize **poly(2)** and **poly(3)** respectively. UV-initiated thiol−ene click reaction is utilized for further modification of **poly(3)**. (B) Isodesmic reaction for ring-opening of **2** and **3** with dimethyl ether and the corresponding ring strain free energies (kcal mol^{-1}) at the SMD$_{(DCM)}$/M06-2X/6-311++G(d,p)//SMD$_{(DCM)}$/M06-L/6-31+G(d,p) level.

polysaccharides with 1,6-α-glycosidic linkages is attractive from a sustainability standpoint since these linkages have demonstrated susceptibility to enzymatic and acidic hydrolysis.[25–27] Despite these advantages, levoglucosan has received considerably less attention in the sustainable polymers field as compared to levoglucosenone,[28–37] another anhydrosugar than can be obtained in small quantities from cellulose pyrolysis.[13]

The cROP of protected levoglucosan derivatives was first reported more than 50 years ago, however the synthetic routes employed had some major drawbacks.[38] These derivatives are generally synthesized from levoglucosan by reaction with alkyl/aryl bromide in the presence of sodium hydride in

dimethylformamide, which is hazardous due to its thermal instability.[39–43] Benzyl and allyl derivatives of levoglucosan have been two of the most widely studied monomers with cROP proceeding at low temperatures in the presence of PF$_5$ or TMSOTf.[44–46] The resulting polymers were de-benzylated/de-allylated for use as polysaccharide mimetics and HPLC stationary phases, respectively.[38,44,47] These polymerization conditions can afford high molecular weight polymers (M_n of 50 kDa), however reaction times were generally long (80 h) and initiators (PF$_5$ & TMSOTf) that are both highly toxic and difficult-to-handle were used.[38,48] Additionally, in these previous studies stereoselective cROP of levoglucosan required rigorous conditions such as high vacuum and very low temperature (−60 °C for the tribenzyl monomer, 0 °C for the triallyl monomer).[38,41,44,45] Overall, identification of alternative low toxicity catalysts for cROP of levoglucosan under mild conditions has remained a challenge, thereby hindering their large scale and sustainable synthesis. This has potentially limited the use of levoglucosan in the sustainable polymers field as compared to other biomass-derived sugars such as levoglucosenone.

Despite the initial investigations in cROP of levoglucosan, the material properties of the resulting polysaccharides have not been characterized and computational insight into the thermodynamics and mechanism of levoglucosan cROP has not been provided. Additionally, very limited work has been done to utilize the rich hydroxyl functionality of levoglucosan for the synthesis of functional polysaccharides. Fu *et al.* synthesized amphiphilic polysaccharides by ring-opening copolymerization of tripropargyl levoglucosan, followed by azide–alkyne cycloaddition modification of the copolymer.[49] However to the best of our knowledge this is the only example of reactive levoglucosan-based materials, providing ample space for the development and characterization of functional levoglucosan polymers. Taken together, these factors have led us to explore methods to improve levoglucosan polymerization conditions while preserving reactive functionalities for polymer modification.

Herein, we report a synthetic platform for stereoregular 1,6-α linked levoglucosan-based polysaccharides with different pendant functional groups. An array of catalysts was screened for the cROP of levoglucosan-based benzyl (Bn) **2** and allyl (All) **3** functional monomers (Fig. 1A) to identify green alternatives. Scandium and bismuth triflate—which are biocompatible and recyclable catalysts—were identified as promising candidates and used for further studies to understand the kinetics, thermodynamics, and mechanism of ring-opening for **2** and **3**. Post-polymerization modification of **poly(3)** was performed with UV-mediated thiol–ene click chemistry to afford functional polymers with a range of solubility and thermal properties. This work paves the way for future development of this renewable platform, enabling facile access to tailored polysaccharides for sustainable polymers to biomaterials applications.

Results and discussion

Monomer synthesis

Monomer **2** was purchased from a commercial supplier and monomer **3** was synthesized on a multi-gram scale using

a modified method for the etherification of starch (75% yield, ESI Sections 2.1 & 9.1†).[50] This synthetic route is safe with easy to handle reagents, employing NaOH as a mild base in dimethyl sulfoxide. We also explored a "greener" synthetic pathway for **3** using NaOH, a phase-transfer catalyst, and water as the reaction medium;[51] the monomer was successfully prepared with this method, albeit in lower yield (36% yield; ESI Section 2.2†).

Screening of cROP conditions

Combined molecular mechanics and density functional theory (DFT) calculations were performed to determine the ring-strain free energies for isodesmic reaction of **2** and **3** with dimethyl ether. Unsurprisingly, both the monomers have comparable ring-strain values, and for both **2** and **3** ring-opening is energetically favored at the 1,6-anhydro linkage over the 1,5-linkage (Fig. 1B), supporting polymerization of **2** and **3**.

To identify less toxic catalysts to promote cROP of **2** and **3**, and to understand the effect of solvent and catalyst loading on cROP of **2** and **3**, a library of polymerization experiments was performed. We initially screened a range of metal and organic catalysts due to their commercial availability, low toxicity, and ability to ring open cyclic ethers for the polymerization of **2** (Fig. S3 and Table S1†).[48,52–58] Cationic initiators BF_3OEt_2 and MeOTf that are conventionally employed for cROP of cyclic acetals were also screened in addition to the array of catalysts for direct comparison.[57,58] All screening reactions took place at room temperature for 72 h in dichloromethane (initial monomer concentration $[M]_0 = 1.0$ mol L^{-1}). Successful catalysts were then used to screen cROP of **3**; two metal triflates $[Sc(OTf)_3$ and $Bi(OTf)_3]$ were identified for cROP of both **2** and **3** (Table 1,

entries 1, 2, 7, 8). Both metal triflates provided comparable conversion to the BF_3OEt_2 and MeOTf controls (Table S2†) and provide the additional benefit of being recyclable (via a simple aqueous extraction) while not releasing corrosive byproducts such as triflic acid commonly released by alkyl triflates.[48] However, these metal triflates have limited solubility in dichloromethane and hence further studies were performed to understand solvent effects.

We investigated the addition of varying quantities of acetonitrile (MeCN), which is a better solvent for the catalyst, in the polymerization mixture. To our surprise, no polymerization occurred when >10% MeCN by volume was present in the reaction medium. Moreover, monomer conversion generally decreased with increasing amount of MeCN from 0–10% (Tables S3 and S4†) and we hypothesize this is due to the better solvation of the ionic active species by MeCN, as reported in the literature.[59,60] We then studied the effect of varying catalyst loading on cROP of **2** and **3** and found that polymerization of both monomers could be conducted at $M(OTf)_3$ loadings as low as 0.5 mol% (Table 1, entries 4, 6, 10). Notably, the pendant groups do not seem to drastically impact conversion, as similar values were observed for both the monomers likely due to their comparable ring-strain (Fig. 1B). With the identified metal triflates, M_w values up to 18.6 kDa for **poly(2)** (DP = 31) and 12.5 kDa for **poly(3)** (DP = 24) could be achieved with moderate dispersities (Table 1, entries 5 and 12). These moderate molecular weights are most likely caused by intermolecular chain transfer and back-biting reactions which are common features in cROP of cyclic acetals.[57] Chain transfer reactions are favored in the cROP of cyclic acetals due to the higher basicity of oxygen atoms in the polymer chain as compared to the

Table 1 Summary of cROP of **2** and **3** under various polymerization conditions

2, R = Bn
3, R = All

poly(2), R = Bn
poly(3), R = All
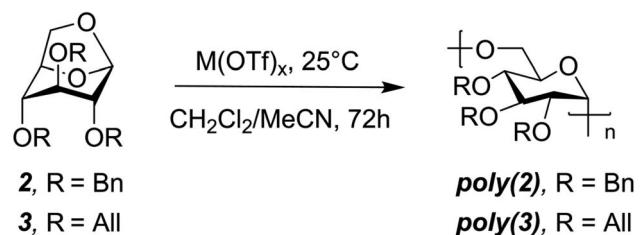
No.	Monomer	Cat.	Solvent CH_2Cl_2 : MeCN	$[M]_0$ (mol L^{-1})	[M] : [cat]	Conv[a] (%)	DP[b]	M_w[b] (g mol^{-1})	Đ[b]
1	2	Sc(OTf)$_3$	100 : 0	1	50 : 1	74	16	11 030	1.6
2	2	Bi(OTf)$_3$	100 : 0	1	50 : 1	84	8	4400	1.3
3	2	Sc(OTf)$_3$	100 : 0	2	100 : 1	82	17	12 200	1.6
4	2	Sc(OTf)$_3$	100 : 0	2	200 : 1	71	27	16 500	1.4
5	2	Sc(OTf)$_3$	99 : 1	2	100 : 1	57	31	18 600	1.4
6	2	Sc(OTf)$_3$	99 : 1	2	200 : 1	34	22	13 400	1.4
7	3	Bi(OTf)$_3$	100 : 0	1	20 : 1	86	13	6100	1.7
8	3	Sc(OTf)$_3$	100 : 0	1	20 : 1	77	12	7900	2.3
9	3	Bi(OTf)$_3$	100 : 0	Bulk	100 : 1	75	24	10 500	1.5
10	3	Bi(OTf)$_3$	100 : 0	Bulk	200 : 1	71	21	9500	1.7
11	3	Bi(OTf)$_3$	99 : 1	2	100 : 1	68	16	6600	1.5
12	3	Bi(OTf)$_3$	99 : 1	Bulk	100 : 1	97	24	12 500	1.9

[a] Monomer conversion determined by ^{1}H NMR spectroscopy. [b] Molecular weight and dispersity determined by SEC-MALS in DMF.

monomer.[57] Moreover, it is hypothesized that metal triflate mediated cROP of levoglucosan derivatives follows a catalytic approach as reported in the literature.[54] In a catalytic approach, one metal triflate molecule catalytically produces a large number of polymer molecules, thereby leading to shorter polymer chains.[54] Since the metal triflate mediated cROP of levoglucosan follows a catalytic approach, calculating a desired or target molecular weight for a given set of polymerization conditions is difficult.

Thermodynamics of polymerization

DFT calculations were employed to provide insights into the mechanism of levoglucosan cROP catalyzed by Bi(OTf)$_3$, Sc(OTf)$_3$, and PF$_5$ (as a control for comparison to previous studies), as well as to understand catalyst efficiency. Various mechanistic pathways were considered (higher energy pathways are provided in the ESI Section 11†), and the lower energy pathway is depicted in Fig. 2A. First, monomer **2** or **3** is activated

by the catalyst to form a thermodynamically stable complex (**I1**). When PF$_5$ is utilized as the catalyst, activation of **2** or **3** is unfavorable relative to the metal triflates due to poor coordination of PF$_5$. This suggests that PF$_5$ exhibits less efficient initiation, leading to the high M_n observed in previous studies.[44,46] After the first step, **I1** undergoes ring opening of 1,6-anhydro linkage to generate the carbenium intermediate **I2** through a TS structure **TS1**, and the activation free energies are similar for monomer **2** or **3** with their respective catalysts, Bi(OTf)$_3$ and Sc(OTf)$_3$ (Fig. 2A, B and S45†). Next, the nucleophilic addition of another molecule of monomer to the electrophilic carbon of intermediate **I2** generates intermediate **I3** *via* a pseudoaxial approach through **TS2**. In this step, the $\Delta G^{\ddagger}$ values for nucleophilic addition of **2** and **3** are similar in all cases (Fig. 2B). Interestingly, it is evident that computed energetics of the nucleophilic addition of monomer to **I2** to form the alternative intermediate structure **I4** (Fig. 2A) indicate it as energetically disfavored (possibly due to the steric hindrance
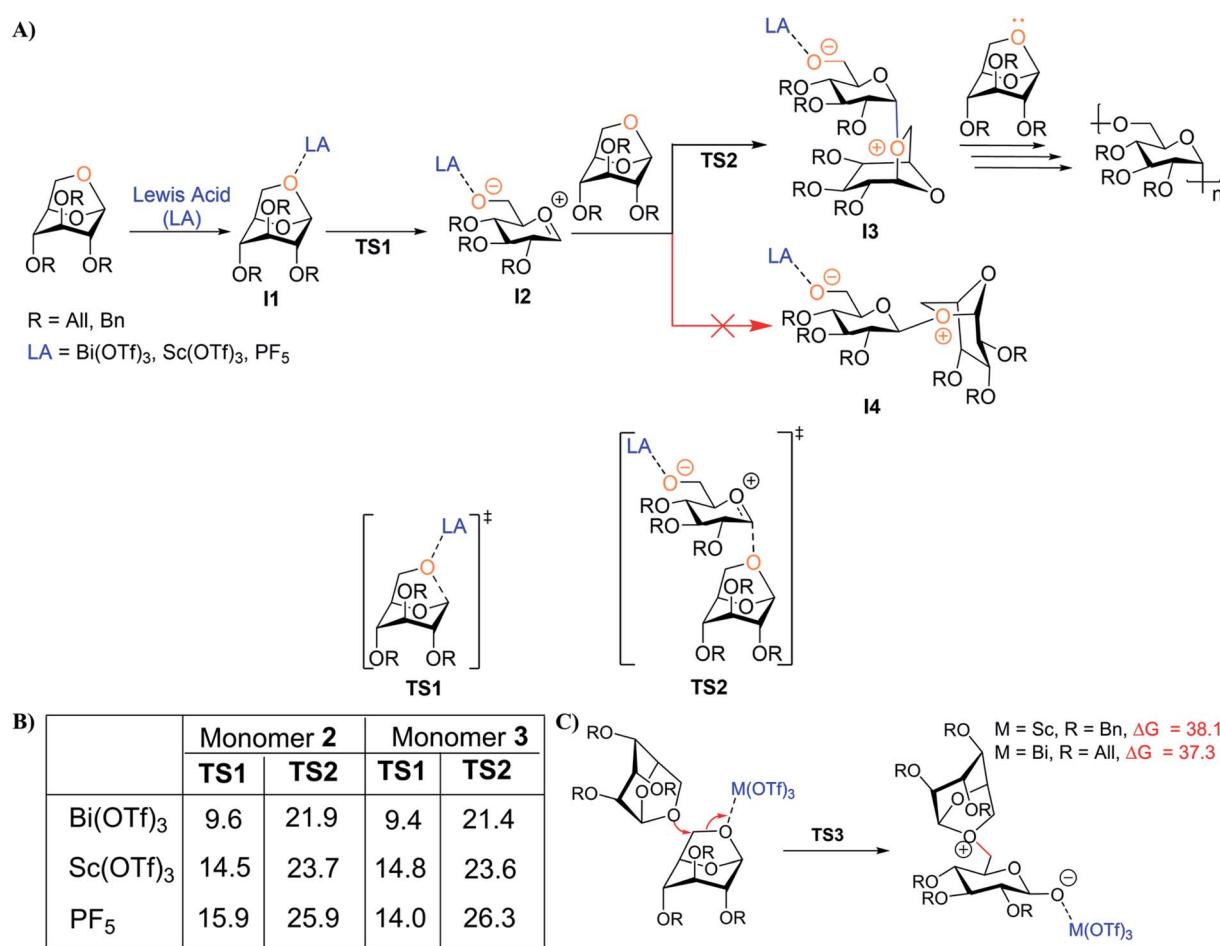
Fig. 2 (A) Key mechanistic steps for cROP of **2** and **3** catalyzed by Lewis acid. Transition-state structures for the ring-opening of 1,6-anhydro linkages (**TS1**) and nucleophilic additions of monomers **2** and **3** (**TS2**) catalyzed by various Lewis acids. Computed energetics indicate that nucleophilic addition of monomers **2** or **3** to **I2** to form intermediate **I4** (pseudo-equatorial approach) is energetically disfavored compared to formation of intermediate **I3** (pseudo-axial approach; Fig. S46†). (B) Table depicting computed energetics in kcal mol^{-1} for key mechanistic steps. (C) Alternative pathway for cROP of **2** catalyzed by Sc(OTf)$_3$ and the cROP of **3** catalyzed by Bi(OTf)$_3$. The corresponding free energies of activation (kcal mol^{-1}) with respect to **I1** at the SMD$_{(DCM)}$/ωB97X-D/def2-TZVP, def2-TZVP|SDD(Bi)//SMD$_{(DCM)}$/M06-L/6-31+G(d,p), LanL2DZ(Bi) level.

between the incoming monomer and catalyst), thereby leading to stereospecific cROP of **2** and **3** (Fig. S46, ESI Section 11.3†). Further, Fig. 2C shows that the monomer addition at C6 of **2** and **3** is energetically disfavored compared to the anomeric carbon. This indicates that cROP proceeds in a regiospecific manner with attack on the anomeric carbon to form 1,6-glycosidic linkages. Finally, computational mechanistic insights also provide some understanding of the moderate molecular weights observed experimentally. Specifically, higher energy barrier pathways may contribute to slower propagation leading to shorter polymer chains (Fig. S48†). Finally, the increase in $\Delta G^{\ddagger}$ and the increase in charge separation between the active ionic species with increased chain length may hinder propagation to high molecular weight polymer.

Polymer stereoregularity

^{1}H NMR analysis of **poly(2)** and **poly(3)** compared to the respective monomers indicates that the polymers possess 1,6-α glycosidic stereoregularity as the anomeric proton resonances (in the β-configuration) appeared at 4.94 ppm (Fig. 3B and D).[41] Additionally ^{13}C NMR of **poly(2)** and **poly(3)** also showed the α configuration as the anomeric carbon resonances appeared at 97.8 ppm and 97.4 ppm, respectively (Fig. S35 and S37†).[41,49] The stereoregularity of the polymers was also confirmed *via* optical rotation measurements. The optical rotation values for **poly(2)** and **poly(3)** were measured to be +91.5 cm^3 dm^{-1} g^{-1} and +84 cm^3 dm^{-1} g^{-1} respectively, with the optical rotation values for **2** and **3** being −31.5 cm^3 dm^{-1} g^{-1} and −45 cm^3 dm^{-1} g^{-1}, respectively. Overall, these results indicate that the cROP of **2** and **3** with metal triflates yields highly stereoregular levoglucosan polymers with 1,6-α glycosidic linkages. Notably, this work

demonstrates that highly stereoregular levoglucosan polymers can be synthesized under mild conditions without the need for an energy intensive process involving high vacuum and low temperatures, as reported previously. ^{1}H NMR analysis also indicates that the alkene functionality in **poly(3)** is intact during cROP with the vinyl proton resonances at 5.91 ppm, 5.27 ppm and 5.14 ppm. The successful synthesis of **poly(3)** while preserving multiple pendant allyl groups will further allow for click-chemistry modifications.

Kinetics of polymerization

Apart from understanding the ring-opening mechanism, we were also interested in investigating the cROP kinetics for each monomer to determine optimum reaction time (ESI Section 5† for details). We observed a short induction period of ∼20 min during cROP of **2** (Table S7 and Fig. S5†), which reaches an equilibrium conversion of 64% in ≤24 h (Fig. 4A). Conversely, cROP of **3** has a much longer induction period of ∼4 h (Table S8†) and reaches an equilibrium conversion of 83% in ≤72 h (Fig. 4B). Remarkably, the induction period for cROP of **3**, as evidenced by ^{1}H NMR spectroscopy, was accompanied with a drastic color change in the solution throughout the 4 h period (Fig. S10 and S11†). We hypothesize that this long cROP induction period of **3** is due to the non-productive coordination of Bi(OTf)₃ with the allylic ether oxygens and the glucopyranose ring oxygen. This was supported by DFT energetics calculations depicting that non-productive coordination of Bi with the allylic ether oxygens and the glucopyranose ring oxygen is favored at multiple locations (Fig. 4C). Furthermore, while comparing **2** and **3**, we find that the relative free energies of binding the M(OTf)₃ to each of these respective oxygen atoms vary slightly
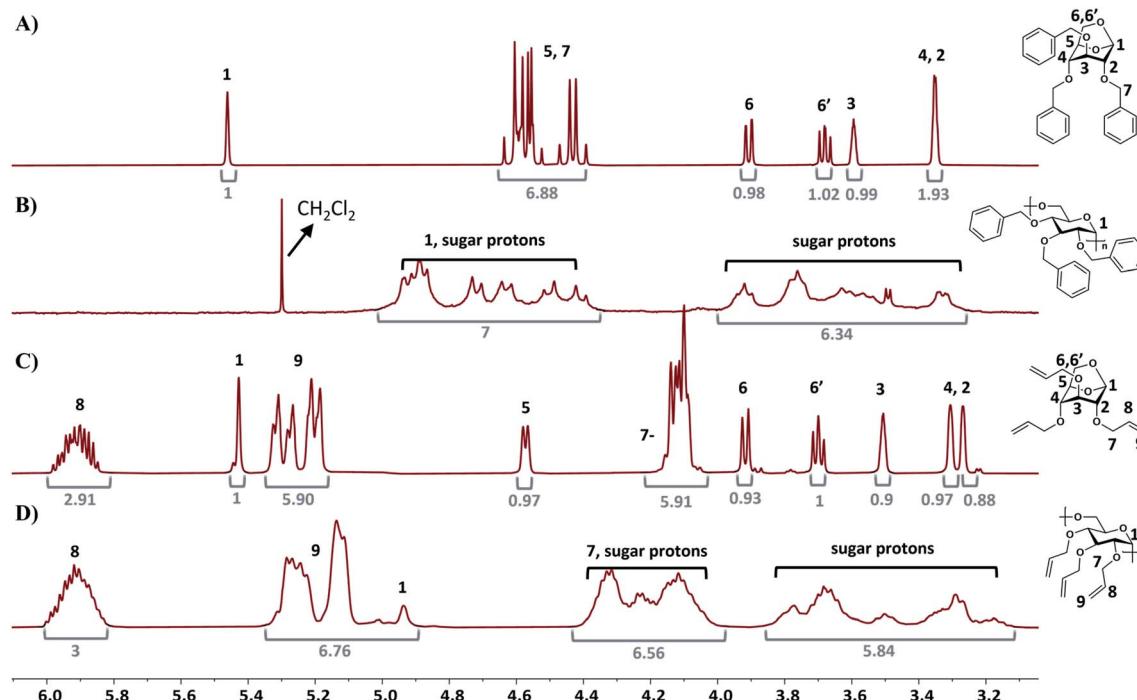
Fig. 3   ^{1}H NMR spectra of (A) monomer **2**, (B) **poly(2)**, (C) monomer **3**, and (D) **poly(3)**. Corresponding integrations are depicted in grey numbers.
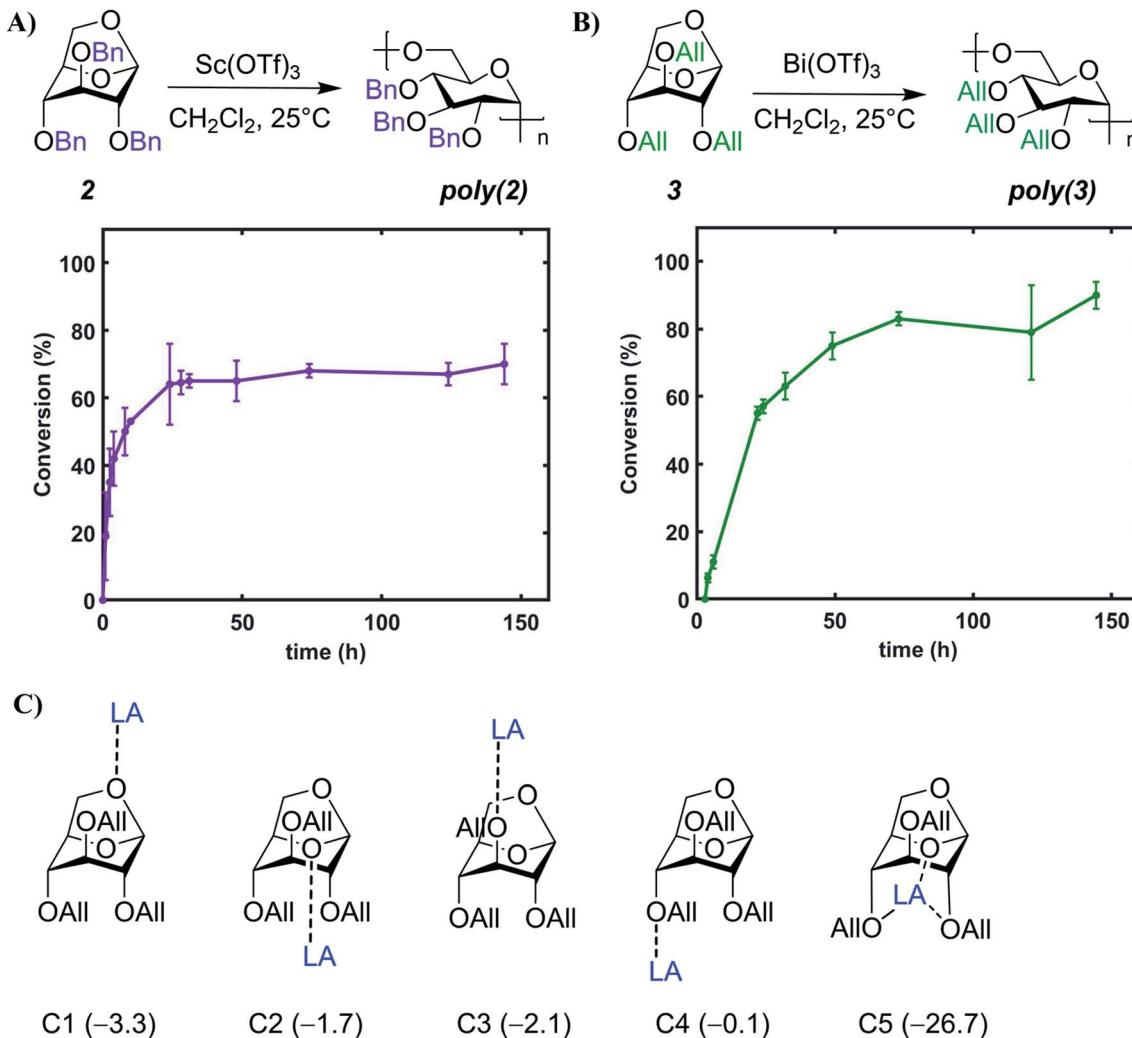
Fig. 4 (A) Conversion-time plot for cROP of **2** with Sc(OTf)$_3$. Polymerization conditions: [**2**]$_0$ = 2 M, **2** : Sc(OTf)$_3$ = 200 : 1. (B) Conversion-time plot for cROP of **3** with Bi(OTf)$_3$. Polymerization conditions: [**3**]$_0$ = 7 M, **3** : Bi(OTf)$_3$ = 100 : 1. Monomer conversion determined by ^{1}H NMR spectroscopy. Error bars based on true values. (C) Coordination modes for monomer **3** with LA (Bi(OTf)$_3$) and the corresponding binding free energies ($\Delta G^{\ddagger}$ in kcal mol^{-1}) are provided in the parenthesis.

(Fig. 4C and S44†). However, the free energy trends and magnitudes are similar across both **2** and **3**. Along with tracking conversion over time, the molar mass and dispersity of the growing polymer chains was also monitored throughout this kinetic study. For **poly(2)**, the M_n increased up to 40% conversion (Fig. S18†), and for **poly(3)** the M_n increased up to 60% conversion (Fig. S19†). Lastly, narrow dispersities were maintained for **poly(2)** throughout the reaction duration (~1.2 to 1.4, Fig. S20†), whereas for **poly(3)** dispersity was higher in the initial stages and gradually decreased to a stable value (~1.5, Fig. S21†).

Thiol–ene post polymerization modification

The allylic pendant groups enable facile post-polymerization modification of **poly(3)**, which we envisioned could serve as a stereo- and regio-regular scaffold for rapid, UV-initiated thiol–ene click reactions for further tailoring polymer properties.[61] Such a renewably-derived and stereoregular scaffold is attractive for many applications such as sustainable polymers and biologically active polymers. Thioglycerol and lauryl mercaptan were chosen as model thiols as they are structurally similar to renewable glycerol and lauryl alcohol.[7,62,63] Additionally, the contrast in hydrophilicity/hydrophobicity of these thiols was expected to provide starkly different properties after modification (Fig. 5A). Real-time Fourier-transform infrared (RT-FTIR) spectroscopy was used to study the kinetics of thiol–ene reactions with **poly(3)**. Fig. 5B depicts the kinetic data for the formation of **poly(4)** and **poly(5)** based on the conversion of the C=C functional groups in **poly(3)**. Both the reactions reach a plateau conversion of >99% in ~1 min, suggesting near full consumption of the allylic pendant groups in **poly(3)**. ^{1}H NMR analysis of purified **poly(4)** and **poly(5)** indicates complete disappearance of vinylic proton signals as shown in Fig. 5C and D. Analysis of **poly(4)** and **poly(5)** by size-exclusion chromatography also
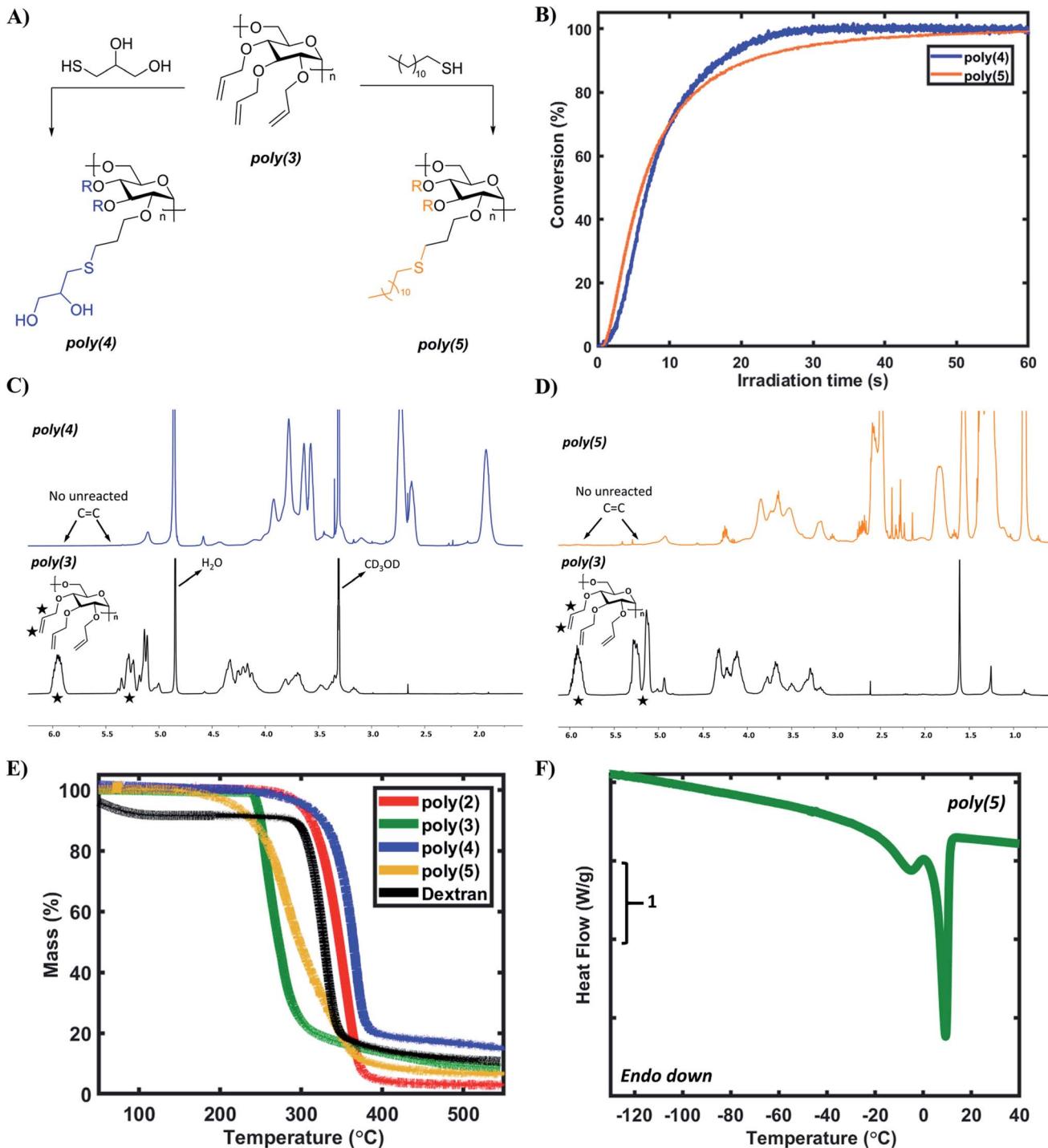
Fig. 5 (A) Schematic depicting post-polymerization modification of **poly(3)** by UV-initiated thiol–ene reaction with 1-thioglycerol and lauryl mercaptan to create **poly(4)** and **poly(5)** respectively. (B) Post-polymerization modification kinetic data depicting conversion of the C=C functional groups in **poly(3)** during UV irradiation. The ratio of thiol to ene groups in both the formulations is 1 : 1. (C) ^{1}H NMR spectrum of **poly(4)** in CD$_3$OD indicating complete disappearance of C=C proton signals. (D) ^{1}H NMR spectrum of **poly(5)** in CDCl$_3$ indicating complete disappearance of C=C proton signals. (E) TGA curves (under N$_2$, 10 °C min^{-1}) of the levoglucosan-based polymers and control dextran. (F) DSC thermogram (second heating, 10 °C min^{-1}) of **poly(5)** depicting the double melting peak.

showed an increase in M_n as compared to **poly(3)**, but some of this increase may be due to fractionation as a result of purification steps (Table S9†). The solubility of synthesized polymers was tested in a range of solvents (Table S10†). As

expected, **poly(4)** and **poly(5)** display starkly different solubility properties, with **poly(4)** being the only water-soluble polymer in the synthesized library.

Thermal properties

Lastly, the thermal properties of the synthesized polysaccharides were examined *via* thermogravimetric analysis (TGA) and differential scanning calorimetry (DSC) to understand thermal stability and thermal transitions respectively. Dextran, a natural and commercial polysaccharide, was used as a control because it also contains 1,6-α-glycosidic linkages and glucopyranose rings. Except for **poly(3)**, each of the homopolymers demonstrated excellent thermal stability with a $T_{d,10\%} >$ 300 °C (Fig. 5E), consistent with the thermal stability of dextran and trimethylated levoglucosan polymer ($T_{d,10\%} = 347$ °C).[19] Comparatively, **poly(3)** had a slightly lower $T_{d,10\%}$ (250 °C), which could be attributed to the fragmentation of pendant allylic ether groups at this temperature, consistent with literature.[64] In general, levoglucosan-based polysaccharides possess excellent thermal stability even at moderate molecular weights, likely due to the rigid glucopyranose ring in the backbone. The glass transition temperature (T_g) of **poly(2)**, **poly(3)**, and **poly(4)** was observed to be 32 °C, 5 °C, and −14 °C, respectively (Fig. S24–S26†); no T_g was observed for **poly(5)** down to −150 °C, which is consistent with other lauryl-pendant polymers.[62,65] The T_g values of **poly(2)**, **poly(3)**, and **poly(5)** are predictably lower than that of the control dextran (199 °C), potentially due to the strong hydrogen bonding between unsubstituted dextran chains. Surprisingly, **poly(4)** exhibited a sub-zero T_g despite the presence of pendant hydroxyl groups, potentially due to the added flexibility of the aliphatic methylene units. Additionally, the T_g for **poly(2)** is lower than that of trimethylated levoglucosan polymer ($T_g \sim 300$ °C).[19] It is hypothesized that this result can be explained based on the steric bulk of pendant groups. As compared to methyl groups, benzyl groups possess higher steric bulk, leading to higher free volume between adjacent polymer chains. A higher free volume will allow polymer chains to slide past each other more easily, thereby resulting in a lower T_g. Overall, DSC analysis demonstrates that the T_g of levoglucosan-based polysaccharides can be tailored based on the identity of the pendant groups, with a remarkable T_g window of >180 °C accessible with the few pendant groups evaluated in this study.

DSC analysis also revealed an interesting double melting peak for **poly(5)** as shown in Fig. 5F ($T_{m1} = -5$ °C, $T_{m2} = 9$ °C). The crystallinity of **poly(5)** is most likely due to lauryl side chain crystallization, also observed in other polymeric systems with lauryl side chains.[62,65] However, the double melting phenomenon could be caused by multiple factors. One explanation is the lamellar thickness model, which attributes the double melting behavior to the presence of lamellae with two different thicknesses.[66–68] Other potential explanations include the crystallization of **poly(5)** chains with varying degrees of side chain functionalization and some extent of polysaccharide backbone crystallization. It is also worth highlighting that even at moderate molecular weights, **poly(3)** offers very high functionality for modification (for $M_n = 6.7$ kDa the number of allyl groups = 72), enabling the facile synthesis of highly functional materials. The high thermal stability, wide range of accessible T_g values, and the potential crystallization phenomena of these derivatives demonstrate that **poly(3)** is an excellent renewable scaffold for post-polymerization reactions to tailor properties to desired applications in a variety of applications. Furthermore, the levoglucosan platform provides easy access to fully functionalized dextran derivatives with the ability to install the desired pendant group both pre- and post-polymerization.

Conclusions

In conclusion, we have synthesized functional stereoregular 1,6-α linked polysaccharides with tunable thermal properties from cellulose-derived levoglucosan *via* cROP and post-polymerization thiol–ene click reactions. Through systematic screening experiments, we have identified green and recyclable metal triflate catalysts for cROP of levoglucosan derivatives under mild conditions. We have also provided kinetic, thermodynamic, and mechanistic insights into cROP of these derivatives. Computational studies reveal that initial ring-opening of levoglucosan derivatives is energetically favored at the 1,6 anhydro linkage and subsequently nucleophilic addition of monomer to the carbenium intermediate leads to 1,6-α glycosidic linkages in a regio- and stereo-specific manner. The allyl-functional polymer has been identified as an excellent scaffold for synthesis of highly functional materials *via* rapid, UV-meditated thiol–ene modifications. Levoglucosan-based polysaccharides generally demonstrate excellent thermal stability and a vast T_g window of >180 °C is accessible with the few pendant groups highlighted in this study. We believe that levoglucosan exhibits great potential as a renewable feedstock for the development of next generation sustainable and biocompatible polymers with tailored properties.

Data availability

The datasets supporting this article are provided in the ESI.†

Author contributions

M. K. P. wrote the manuscript and performed all experimental studies and data analysis. Y. R. performed all computational studies and contributed to the computation related text and figures in the manuscript. D. J. S. provided mentorship and edited the manuscript. C. J. C. provided mentorship for computational studies and edited the computation related parts of the manuscript. C. J. E. and T. M. R. provided mentorship, research direction, and edited the manuscript.

Conflicts of interest

There are no conflicts to declare.

Acknowledgements

References

1 R. Geyer, in *Plastic Waste and Recycling*, ed. Trevor M. Letcher, 2020, pp. 13–32.

2 M. Hong and E. Y.-X. Chen, Future Directions for Sustainable Polymers, *Trends Chem.*, 2019, **1**, 148–152.

3 L. A. Lucia, Lignocellulosic biomass: A potential feedstock to replace petroleum, *BioResources*, 2008, **3**, 981–982.

4 J. C. Serrano-Ruiz, R. Luque and A. Sepúlveda-Escribano, Transformations of biomass-derived platform molecules: From high added-value chemicals to fuels via aqueous-phase processing, *Chem. Soc. Rev.*, 2011, **40**, 5266–5281.

5 O. Olatunji, S. Akinlabi and N. Madushele in *Valorization of Biomass to Value-Added Commodities, Springer Nature Switzerland AG*, ed. A. O. A. M. O. Daramola, 2020, pp. 3–20.

6 R. M. O'dea, J. A. Willie and T. H. Epps, 100th Anniversary of Macromolecular Science Viewpoint: Polymers from Lignocellulosic Biomass. Current Challenges and Future Opportunities, *ACS Macro Lett.*, 2020, **9**, 476–493.

7 F. H. Isikgor and C. R. Becer, Lignocellulosic biomass: a sustainable platform for the production of bio-based chemicals and polymers, *Polym. Chem.*, 2015, **6**, 4497–4559.

8 C. H. Zhou, X. Xia, C. X. Lin, D. S. Tong and J. Beltramini, Catalytic conversion of lignocellulosic biomass to fine chemicals and fuels, *Chem. Soc. Rev.*, 2011, **40**, 5588–5617.

9 Z. Zhang, J. Song and B. Han, Catalytic Transformation of Lignocellulose into Chemicals and Fuel Products in Ionic Liquids, *Chem. Rev.*, 2017, **117**, 6834–6880.

10 N. Brun, P. Hesemann and D. Esposito, Expanding the biomass derived chemical space, *Chem. Sci.*, 2017, **8**, 4724–4738.

11 S. Maduskar, V. Maliekkal, M. Neurock and P. J. Dauenhauer, On the Yield of Levoglucosan from Cellulose Pyrolysis, *ACS Sustain. Chem. Eng.*, 2018, **6**, 7017–7025.

12 M. R. Rover, A. Aui, M. M. Wright, R. G. Smith and R. C. Brown, Production and purification of crystallized levoglucosan from pyrolysis of lignocellulosic biomass, *Green Chem.*, 2019, **21**, 5980–5989.

13 I. Itabaiana Junior, M. Avelar Do Nascimento, R. O. M. A. De Souza, A. Dufour and R. Wojcieszak, Levoglucosan: A promising platform molecule?, *Green Chem.*, 2020, **22**, 5859–5880.

14 I. G. Hakeem, P. Halder, M. H. Marzbali, S. Patel, S. Kundu, J. Paz-Ferreiro, A. Surapaneni and K. Shah, Research progress on levoglucosan production via pyrolysis of lignocellulosic biomass and its effective recovery from bio-oil, *J. Environ. Chem. Eng.*, 2021, **9**, 105614.

15 J. Wang, Z. Lu and A. Shah, Techno-economic analysis of levoglucosan production via fast pyrolysis of cotton straw in China, *Biofuels, Bioprod. Biorefining*, 2019, **13**, 1085–1097.

16 A. Zheng, T. Chen, J. Sun, L. Jiang, J. Wu, Z. Zhao, Z. Huang, K. Zhao, G. Wei, F. He and H. Li, Toward Fast Pyrolysis-Based Biorefinery: Selective Production of Platform Chemicals from Biomass by Organosolv Fractionation Coupled with Fast Pyrolysis, *ACS Sustain. Chem. Eng.*, 2017, **5**, 6507–6516.

17 K. Wu, H. Wu, H. Zhang, B. Zhang, C. Wen, C. Hu, C. Liu and Q. Liu, Enhancing levoglucosan production from waste biomass pyrolysis by Fenton pretreatment, *Waste Manag.*, 2020, **108**, 70–77.

18 S. Penczek, P. Kubisa and K. Matyjaszewski, Bicyclic Monomers in Cationic Ring-Opening Polymerization, *Adv. Polym. Sci.*, 1985, 139–176.

19 D. Yoshida and T. Yoshida, Elucidation of High Ring-Opening Polymerizability of Methylated 1,6-Anhydro Glucose, *J. Polym. Sci. Part A Polym. Chem.*, 2009, **47**, 1013–1022.

20 T. Yoshida, Synthesis of polysaccharides having specific biological activities, *Prog. Polym. Sci.*, 2001, **26**, 379–441.

21 M. Grinstaff, R. Xiao and M. W. Grinstaff, Chemical Synthesis of Polysaccharides and Polysaccharide Mimetics Progress in Polymer Science Chemical synthesis of polysaccharides and polysaccharide mimetics, *Prog. Polym. Sci.*, 2017, **74**, 78–116.

22 G. L. Gregory, E. M. Lopez-Vidal and A. Buchard, Polymers from sugars: cyclic monomer synthesis, ring-opening polymerisation, material properties and applications, *Chem. Commun.*, 2017, **53**, 2198–2217.

23 A. S. Balijepalli and M. W. Grinstaff, Poly-Amido-Saccharides (PASs): Functional Synthetic Carbohydrate Polymers Inspired by Nature, *Acc. Chem. Res.*, 2020, **53**, 2167–2179.

24 M. Varghese, R. S. Rokosh, C. A. Haller, S. L. Chin, J. Chen, E. Dai, R. Xiao, E. L. Chaikof and M. W. Grinstaff, Sulfated poly-amido-saccharides (sulPASs) are anticoagulants: In vitro and in vivo, *Chem. Sci.*, 2021, **12**, 12719–12725.

25 K. Kobayashi, H. Sumitomo and H. Ichikawa, Regioselectively Modified Stereoregular Polysaccharides. 8. Synthesis and Functions of Partially 3-O-Octadecylated (1→ 6) -α-D- Glucopyranans, *Macromolecules*, 1986, **19**, 529–535.

26 M. D. Gallovic, S. Bandyopadhyay, H. Borteh, D. G. Montjoy, M. A. Collier, K. J. Peine, B. E. Wyslouzil, E. M. Bachelder and K. M. Ainslie, Microparticles formulated from a family of novel silylated polysaccharides demonstrate inherent immunostimulatory properties and tunable hydrolytic degradability, *J. Mater. Chem. B*, 2016, **4**, 4302–4312.

27 S. Iqbal, R. Marchetti, A. Aman, A. Silipo, S. A. U. Qader and A. Molinaro, Enzymatic and acidic degradation of high molecular weight dextran into low molecular weight and its characterizations using novel Diffusion-ordered NMR spectroscopy, *Int. J. Biol. Macromol.*, 2017, **103**, 744–750.

28 F. Diot-Néant, E. Rastoder, S. A. Miller and F. Allais, Chemo-Enzymatic Synthesis and Free Radical Polymerization of Renewable Acrylate Monomers from Cellulose-Based Lactones, *ACS Sustain. Chem. Eng.*, 2018, **6**, 17284–17293.

29 T. Debsharma, Y. Yagci and H. Schlaad, Cellulose-Derived Functional Polyacetal by Cationic Ring-Opening Polymerization of Levoglucosenyl Methyl Ether, *Angew. Chem., Int. Ed.*, 2019, **58**, 18492–18495.

30 T. Debsharma, F. N. Behrendt, A. Laschewsky and H. Schlaad, Ring-Opening Metathesis Polymerization of Biomass-Derived Levoglucosenol, *Angew. Chemie*, 2019, **131**, 6790–6793.

31 P. Ray, T. Hughes, C. Smith, M. Hibbert, K. Saito and G. P. Simon, Development of bio-acrylic polymers from Cyrene™: Transforming a green solvent to a green polymer, *Polym. Chem.*, 2019, **10**, 3334–3341.

32 K. Kaya, T. Debsharma, H. Schlaad and Y. Yagci, Cellulose-based polyacetals by direct and sensitized photocationic ring-opening polymerization of levoglucosenyl methyl ether, *Polym. Chem.*, 2020, **11**, 6884–6889.

33 S. Fadlallah, A. A. M. Peru, A. L. Flourat and F. Allais, A straightforward access to functionalizable polymers through ring-opening metathesis polymerization of levoglucosenone-derived monomers, *Eur. Polym. J.*, 2020, **138**, 109980.

34 M. G. Banwell, X. Liu, L. A. Connal and M. G. Gardiner, Synthesis of Functionally and Stereochemically Diverse Polymers via Ring-Opening Metathesis Polymerization of Derivatives of the Biomass-Derived Platform Molecule Levoglucosenone Produced at Industrial Scale, *Macromolecules*, 2020, **53**, 5308–5314.

35 S. Fadlallah, A. A. M. Peru, L. Longé and F. Allais, Chemo-enzymatic synthesis of a levoglucosenone-derived bi-functional monomer and its ring-opening metathesis polymerization in the green solvent Cyrene™, *Polym. Chem.*, 2020, **11**, 7471–7475.

36 F. Diot-Néant, L. Mouterde, S. Fadlallah, S. A. Miller and F. Allais, Sustainable Synthesis and Polycondensation of Levoglucosenone-Cyrene-Based Bicyclic Diol Monomer: Access to Renewable Polyesters, *ChemSusChem*, 2020, **13**, 2613–2620.

37 T. Debsharma, B. Schmidt, A. Laschewsky and H. Schlaad, Ring-Opening Metathesis Polymerization of Unsaturated Carbohydrate Derivatives: Levoglucosenyl Alkyl Ethers, *Macromolecules*, 2021, **54**, 2720–2728.

38 E. R. Ruckel and C. Schuerch, Preparation of High Polymers from l,6-Anhydro-2,3,4-tri-O-Substituted β-D-Glucopyranose, *J. Org. Chem.*, 1966, **31**, 2233–2239.

39 Y. Du Hongmei Liu, S. Cheng, J. Liu, Y. Du and Z. Bai, Synthesis of Pentasaccharide and Heptasaccharide Derivatives and Their Effects on Plant Growth, *J. Agric. Food Chem.*, 2008, **56**, 5634–5638.

40 A. Fürstner, M. Albert, J. Mlynarski, M. Matheu and E. DeClercq, Structure Assignment, Total Synthesis, and Antiviral Evaluation of Cycloviracin B1, *J. Am. Chem. Soc.*, 2003, **125**, 13132–13142.

41 T. Kakuchi, A. Kusuno, M. Miura and H. Kaga, Cationic ring-opening polymerization of 1,6-anhydro-2,3,4-tri-O-allyl-b-D-glucopyranose as a convenient synthesis of dextran, *Macromol. Rapid Commun.*, 2000, **21**, 1003–1006.

42 T. Laird, Special feature section: Safety of chemical processes, *Org. Process Res. Dev.*, 2002, **6**, 876.

43 Q. Yang, M. Sheng, J. J. Henkelis, S. Tu, E. Wiensch, H. Zhang, Y. Zhang, C. Tucker and D. E. Ejeh, Explosion Hazards of Sodium Hydride in Dimethyl Sulfoxide, N, N-Dimethylformamide, and N, N-Dimethylacetamide, *Org. Process Res. Dev.*, 2019, **23**, 2210–2217.

44 T. Uryu, H. Tachikawa, K.-I. Ohaku, K. Terui and K. Matsuzaki, Synthesis of 2,3,4-tri-O-benzyl-[1→6]-α-D-glucopyranan and [1→6]-α-D-glucopyranan with high molecular weight by polymerization of 1,6-anhydro-2,3,4-tri-O-benzyl-β-D-glucopyranose, *Makromol. Chem.*, 1977, **178**, 1929–1940.

45 J. Zachoval and C. Schuerch, Steric Control in the Polymerization of 1,6-Anhydro-B-D-glucopyranose Derivatives, *J. Am. Chem. Soc.*, 1969, **91**, 1165–1169.

46 T. Kakuchi, A. Kusuno, M. Mori, T. Satoh, M. Miura, M. Sharfuddin and H. Kaga, Precision synthesis of (1→6)-α-D-glucopyranan by cationic ring-opening polymerization of 1,6-anhydro-2,3,4-tri-O-allyl-β-D-glucopyranose, *Macromol. Symp.*, 2002, **181**, 101–106.

47 A. Kusuno, M. Mori, T. Satoh, M. Miura, H. Kaga and T. Kakuchi, Enantioseparation properties of (1→6)-α-D-glucopyranan and (1→6)-α-D-mannopyranan tris(phenylcarbamate)s as chiral stationary phases in HPLC, *Chirality*, 2002, **14**, 498–502.

48 L. You, T. E. Hogen-Esch, Y. Zhu, J. Ling and Z. Shen, Brønsted acid-free controlled polymerization of tetrahydrofuran catalyzed by recyclable rare earth triflates in the presence of epoxides, *Polymer*, 2012, **53**, 4112–4118.

49 L. Fu, L. Li, J. Wang, K. Knickelbein, L. Zhang, I. Milligan, Y. Xu, K. O'Hara, L. Bitterman and W. Du, Synthesis of clickable amphiphilic polysaccharides as nanoscopic assemblies, *Chem. Commun.*, 2014, **50**, 12742–12745.

50 N. Teramoto, T. Motoyama, R. Yosomiya and M. Shibata, Synthesis, thermal properties, and biodegradability of propyl-etherified starch, *Eur. Polym. J.*, 2003, **39**, 255–261.

51 C. Lorenzini, D. L. Versace, C. Gaillet, C. Lorthioir, S. Boileau, E. Renard and V. Langlois, Hybrid networks derived from isosorbide by means of thiol-ene photoaddition and sol-gel chemistry, *Polymer*, 2014, **55**, 4432–4440.

52 D. J. Saxon, M. Nasiri, M. Mandal, S. Maduskar, P. J. Dauenhauer, C. J. Cramer, A. M. Lapointe and T. M. Reineke, Architectural Control of Isosorbide-Based Polyethers via Ring-Opening Polymerization, *J. Am. Chem. Soc.*, 2019, **141**, 5107–5111.

53 M. Lahcini, H. Qayouh, T. Yashiro, S. M. Weidner and H. R. Kricheldorf, Bismuth-triflate-catalyzed polymerizations of ε-caprolactone, *Macromol. Chem. Phys.*, 2011, **212**, 583–591.

54 N. Nomura, A. Taira, T. Tomioka and M. Okada, Catalytic approach for cationic living polymerization: Sc(OTf)3-catalyzed ring-opening polymerization of lactones, *Macromolecules*, 2000, **33**, 1497–1499.

55 A. E. Neitzel, T. J. Haversang and M. A. Hillmyer, Organocatalytic Cationic Ring-Opening Polymerization of a Cyclic Hemiacetal Ester, *Ind. Eng. Chem. Res.*, 2016, **55**, 11747–11755.

56 M. Helou, J. M. Brusson, J. F. Carpentier and S. M. Guillaume, Functionalized polycarbonates from dihydroxyacetone: Insights into the immortal ring-opening polymerization of 2,2-dimethoxytrimethylene carbonate, *Polym. Chem.*, 2011, **2**, 2789–2795.

57 P. Kubisa and J. P. Vairon, Ring-Opening Polymerization of Cyclic Acetals, *Polymer Science: A Comprehensive Reference 10 Vol. Set*, 2012, vol. 4, pp. 183–211.

58 B. T. Whiting and G. W. Coates, Synthesis and Polymerization of Bicyclic Ketals : A Practical Route to High-Molecular Weight Polyketals, *J. Am. Chem. Soc.*, 2013, **135**(30), 10974–10977.

59 M. Kawalec, M. Śmiga-Matuszowicz and P. Kurcok, Counterion and solvent effects on the anionic polymerization of β-butyrolactone initiated with acetic acid salts, *Eur. Polym. J.*, 2008, **44**, 3556–3563.

60 G. Odian, *Principles of Polymerization*, John Wiley & Sons, 2004.

61 C. E. Hoyle and C. N. Bowman, Thiol-ene click chemistry, *Angew. Chem., Int. Ed.*, 2010, **49**, 1540–1573.

62 H. Sajjad, W. B. Tolman and T. M. Reineke, Block Copolymer Pressure-Sensitive Adhesives Derived from Fatty Acids and Triacetic Acid Lactone, *ACS Appl. Polym. Mater.*, 2020, **2**, 2719–2728.

63 S. Wang, S. Vajjala Kesava, E. D. Gomez and M. L. Robertson, Sustainable thermoplastic elastomers derived from fatty acids, *Macromolecules*, 2013, **46**, 7202–7212.

64 T. K. Vardareli, S. Keskin and A. Usanmaz, Thermal degradation of poly(allyl methacrylate) by mass spectroscopy and TGA, *J. Macromol. Sci. Part A Pure Appl. Chem.*, 2006, **43**, 1569–1581.

65 D. J. Saxon, E. A. Gormong, V. M. Shah and T. M. Reineke, Rapid Synthesis of Chemically Recyclable Polycarbonates from Renewable Feedstocks, *ACS Macro Lett.*, 2021, **10**, 98–103.

66 A. Alizadeh, L. Richardson, J. Xu, S. McCartney, H. Marand, Y. W. Cheung and S. Chum, Influence of structural and topological constraints on the crystallization and melting behavior of polymers. 1. Ethylene/1-octene copolymers, *Macromolecules*, 1999, **32**, 6221–6235.

67 C. Schick, Differential scanning calorimetry (DSC) of semicrystalline polymers, *Anal. Bioanal. Chem.*, 2009, **395**, 1589–1611.

68 O. P. Bajpai, S. Panja, S. Chattopadhyay and D. K. Setua, *Process-structure-property relationships in nanocomposites based on piezoelectric-polymer matrix and magnetic nanoparticles*, Elsevier Ltd., 2015.